The CYCLIN-DEPENDENT KINASE Module of the Mediator Complex Promotes Flowering and Reproductive Development in Pea[1][OPEN]

A. S. M. Mainul Hasan, Jacqueline K. Vander Schoor, Valerie Hecht, and James L. Weller[2,3]

School of Natural Sciences, University of Tasmania, Hobart, Tasmania 7001, Australia

ORCID IDs: 0000-0003-3201-395X (A.S.M.M.H.); 0000-0002-3539-3356 (V.H.); 0000-0003-2423-8286 (J.L.W.).

Control of flowering time has been a major focus of comparative genetic analyses in plant development. This study reports on a forward genetic approach to define previously uncharacterized components of flowering control pathways in the long-day legume, pea (*Pisum sativum*). We isolated two complementation groups of late-flowering mutants in pea that define two uncharacterized loci, *LATE BLOOMER3* (*LATE3*) and *LATE4*, and describe their diverse effects on vegetative and reproductive development. A map-based comparative approach was employed to identify the underlying genes for both loci, revealing that that LATE3 and LATE4 are orthologs of CYCLIN DEPENDENT KINASE8 (CDK8) and CYCLIN C1 (CYCC1), components of the CDK8 kinase module of the Mediator complex, which is a deeply conserved regulator of transcription in eukaryotes. We confirm the genetic and physical interaction of LATE3 and LATE4 and show that they contribute to the transcriptional regulation of key flowering genes, including the induction of the florigen gene *FTa1* and repression of the floral repressor *LF*. Our results establish the conserved importance of the CDK8 module in plants and provide evidence for the function of CYCLIN C1 orthologs in the promotion of flowering and the maintenance of normal reproductive development.

The initiation of flowering is one of the key developmental changes in the plant life cycle and is regulated by different environmental factors and endogenous cues. Evidence from Arabidopsis (*Arabidopsis thaliana*) indicates that it is a highly complex process, regulated by hundreds of genes through transcriptional, post-transcriptional, and epigenetic pathways (Bratzel and Turck, 2015; Song et al., 2015; Whittaker and Dean, 2017). One well-known control point is the *FT* gene, which encodes a small protein that is formed in leaf vasculature and moves through the phloem to the shoot apical meristem, where it interacts with the basic leucine zipper (bZIP) domain transcription factor FD. This complex then activates transcription of floral meristem identity genes such as MADS box genes *LEAFY* (*LFY*) and *APETALA1* (*AP1*) via *SUPPRESSOR OF OVEREXPRESSION OF CONSTANS1* (*SOC1*), leading to initiation of flowering (Wigge et al., 2005; Andrés and Coupland, 2012).

There is growing appreciation of the importance of regulatory mechanisms at the *FT* locus. The effects of many different environmental and endogenous factors on flowering are integrated through effects on *FT* expression (Andrés and Coupland, 2012; Song et al., 2015; Cho et al., 2017), and numerous proteins have been reported to associate with the *FT* promoter and other regulatory regions in or near the *FT* gene, including generalist transcription factors, transcriptional co-regulators, and histone-modifying proteins (Bratzel and Turck, 2015; Luo et al., 2018). However, relatively little detail is known about specific mechanisms and interactions by which these factors regulate *FT* transcription.

Transcriptional regulation is also critical at many other different points in the flowering time network. For example, in addition to direct regulation of and by *FT* itself, pathways upstream and downstream also feature transcriptional control. Examples include the circadian and light control of the *FT* activator *CONSTANS* (Shim et al., 2017), repression of the *FT* repressor *FLC* in response to cold (Whittaker and Dean, 2017), and the mutually repressive interactions that establish organ identity and govern the patterning of inflorescences and flowers (Wagner, 2017). In addition to these largely flowering-specific factors, many general transcriptional and epigenetic regulators have also been identified from their effects on flowering time and reproductive development or have been shown to participate in these processes. These include NUCLEAR FACTOR-Y, the TOPLESS corepressor, and polycomb

[1]This project was funded in part by the Australian Research Council (grants DP120101241 and DP160100793 to J.L.W.).

[2]Author for contact: jim.weller@utas.edu.au

[3]Senior author

The author responsible for distribution of materials integral to the findings presented in this article in accordance with the policy described in the Instructions for Authors (www.plantphysiol.org) is: James L. Weller (jim.weller@utas.edu.au).

J.L.W. conceived the project; A.S.M.M.H., V.H., J.K.V.S. and J.L.W. designed and performed the experiments and analyzed data; J.L.W. and V.H. supervised the experiments; and A.S.M.M.H. and J.L.W. wrote the article.

[OPEN]Articles can be viewed without a subscription.

www.plantphysiol.org/cgi/doi/10.1104/pp.19.01173

repressive complex2 (Causier et al., 2012; Eom et al., 2018).

In comparison to Arabidopsis, less is known about flowering time control in other plant groups. Loci controlling natural variation for flowering time have been identified across many major crop species (Fjellheim et al., 2014; Blümel et al., 2015; Brambilla et al., 2017; Cao et al., 2017; Higuchi, 2018), and such studies have highlighted aspects of regulation that are deeply conserved but others that may be confined to specific groups. As in Arabidopsis, flowering time control involves both specific pathways and general transcriptional and chromatin regulators (Shi et al., 2015; Brambilla et al., 2017). However, our understanding of the mechanisms controlling flowering time is still relatively limited in many species.

Legumes are a major plant group that includes many crop plants that display wide, agriculturally relevant variation in flowering time (Weller and Ortega, 2015). They include both short-day (SD) and long-day (LD) responsive species for which soybean (*Glycine max*) and pea (*Pisum sativum*) have been prominent examples. Characterization of induced mutants and natural variation in these and other species have been useful in defining flowering-associated loci (Weller and Ortega, 2015; Cao et al., 2017), and reverse genetics is increasingly employed for defining specific gene functions (e.g. Laurie et al., 2011; Berbel et al., 2012; Cai et al., 2018). A forward genetic strategy in pea has previously identified a number of loci that control flowering time through primary roles in light perception and signaling, circadian clock function, and regulation and function of florigen genes (e.g. Sussmilch et al., 2015; Weller and Ortega, 2015; Ridge et al., 2016). In this study, we have characterized two additional loci, *LATE BLOOMER3* (*LATE3*) and *LATE4*, that have extremely late-flowering mutant phenotypes and other pleiotropic effects on vegetative and reproductive development. We identify these genes as likely components of the Mediator transcriptional coregulator complex and present evidence that their effects on flowering may in part result from effects on the transcription of *FT* and *TFL1* homologs.

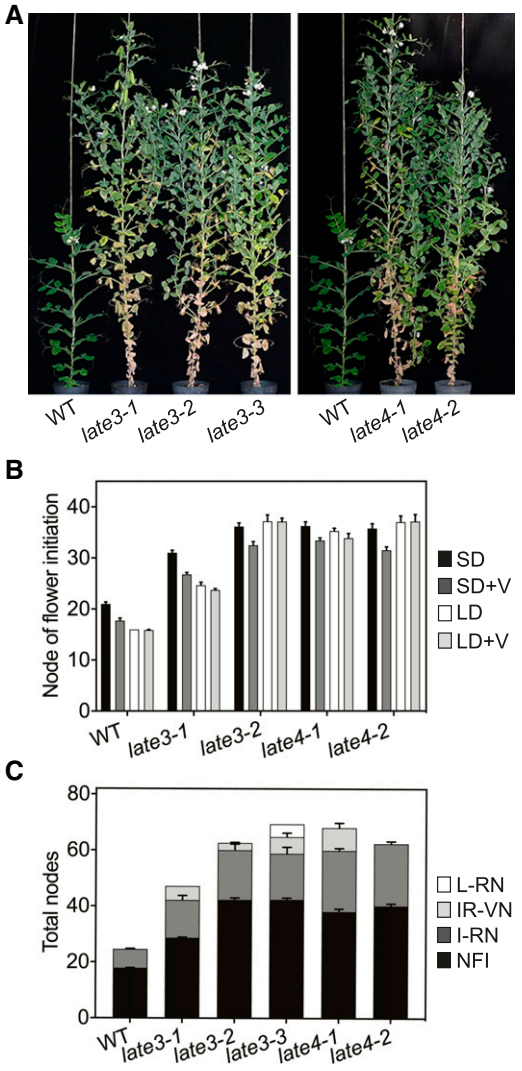

Figure 1. Mutations at *LATE3* and *LATE4* loci delay flowering and prolong the reproductive phase. A, Representative wild-type (WT; NGB5839), *late3*, and *late4* plants grown under 16-h long-day conditions. To account for the disparity in flowering time, this image compares WT and mutants at 62 and 130 d after sowing, respectively. B and C, Effect of photoperiod and vernalization on flowering initiation in WT, *late3*, and *late4*, mutant plants. Data represent mean ± SE for $n = 6$ to 8 plants. +V, vernalization; NFI, node of flower initiation; I-RN, initial reproductive nodes; IR-VN, inflorescence reverted-vegetative nodes; L-RN, later reproductive nodes.

RESULTS

LATE3 and *LATE4* Promote Flowering and Impair Responsiveness to Photoperiod

Among a number of flowering-time mutants generated through ethylmethanesulfonate mutagenesis (Hecht et al., 2007), we identified five similar fully recessive mutants that showed a substantial delay in flowering and maturity under LD conditions. These mutants defined two genetic loci: *LATE BLOOMER3* (*LATE3*), with three mutant alleles, and *LATE4*, with two alleles (Fig. 1A). Four of the five mutants flowered equivalently late at around node 35 in comparison to wild-type line NGB5839, which flowered at around node 16 under LD (Fig. 1B). Only the *late3-1* mutant was notably earlier in flowering than the other mutants. Overall, the *late3* and *late4* late-flowering phenotype was notably more severe than that of other previously described late-flowering mutants at the *PHYTOCHROME A* (*PHYA*), *LATE1*, and *LATE2* loci (Ridge et al., 2016). We also examined the response of *late3* and *late4* mutants to photoperiod and vernalization. Whereas wild type and *late3-1* flowered earlier under LD than under SD, other mutants at both loci showed no effect of photoperiod on flowering initiation (Fig. 1B). By contrast, all mutant lines showed a small

but significant response to vernalization under SD ($P < 0.05$ in all cases), similar to wild type (Fig. 1B).

LATE3 and *LATE4* Have Pleiotropic Effects throughout Reproductive Development

The *late3* and *late4* mutants also shared a number of additional defects that differed from those seen in previously described flowering-time mutants in pea. The most conspicuous of these was an extreme delay in maturity and senescence illustrated by the substantial increase in the number of reproductive nodes relative to wild type (initial reproductive nodes; $P < 0.05$ for all comparisons; Fig. 1C). This was accompanied by, and probably in part enhanced by, numerous defects in other aspects of reproductive development, including flower and inflorescence formation, flower fertility, pod formation, and seed content.

For example, whereas most secondary inflorescences in *late3* and *late4* mutants had a normal structure and developed to produce open flowers, a substantial minority showed growth defects in which they remained arrested or aborted at an early growth stage (Supplemental Fig. S1, A–C). Other secondary inflorescences displayed defects in identity, failing to suppress leaflet and bract formation and/or exhibiting reduced determinacy (Supplemental Fig. S1, A–C).

Where flowers did develop fully and open, other defects were evident. Some had abnormal organ morphology and number, and in the more severe mutants, pollen abundance was low and most flowers were sterile, with pods forming on only a small proportion of flowers (Fig. 2A). During the process of genetic analysis, it became apparent that the success rate of crosses made with wild-type pollen onto *late3* and *late4* mutants was also markedly reduced, suggesting that the reduced fertility derived from both paternal and maternal defects. When pods were formed, they often arrested in a partially developed state, and where they developed fully, they were generally shorter and contained fewer, smaller seeds (Fig. 2, B–D; Supplemental Fig. S2).

Finally, all mutants showed variable expression of these defects across the reproductive phase, with zones of more advanced development followed by stages of greater impairment. In addition, after forming 12 to 20 reproductive nodes, the mutants reverted to production of vegetative axillary buds, and in some cases subsequently reinitiated reproductive development at later nodes (Fig. 1C; Supplemental Fig. S1, D–E). Overall, provided they remained disease free, *late3* and *late4* mutant plants under glasshouse LD continued to grow for more than 6 months without signs of terminal senescence, in contrast to wild type, which generally reached maturity within 90 d.

LATE3 and *LATE4* Also Affect Aspects of Vegetative Development

Initial observations in segregating progenies suggested *late3* and *late4* mutants could also be distinguished from wild type early in development, on the basis of a number of vegetative growth traits. Both *late3* and *late4* mutants showed significant reduction in leaflet area, petiole and proximal rachis length (Supplemental Fig. S3, A–C; both $P < 0.0001$), and stem diameter compared to wild type (Supplemental Fig. S3E; $P < 0.0001$). By 4 weeks after sowing, mutants also exhibited lower shoot and root dry weight in comparison to wild type (Supplemental Fig. S3, F and G; both $P < 0.05$). The *late3* and *late4* mutants also showed a substantial increase in shoot branching relative

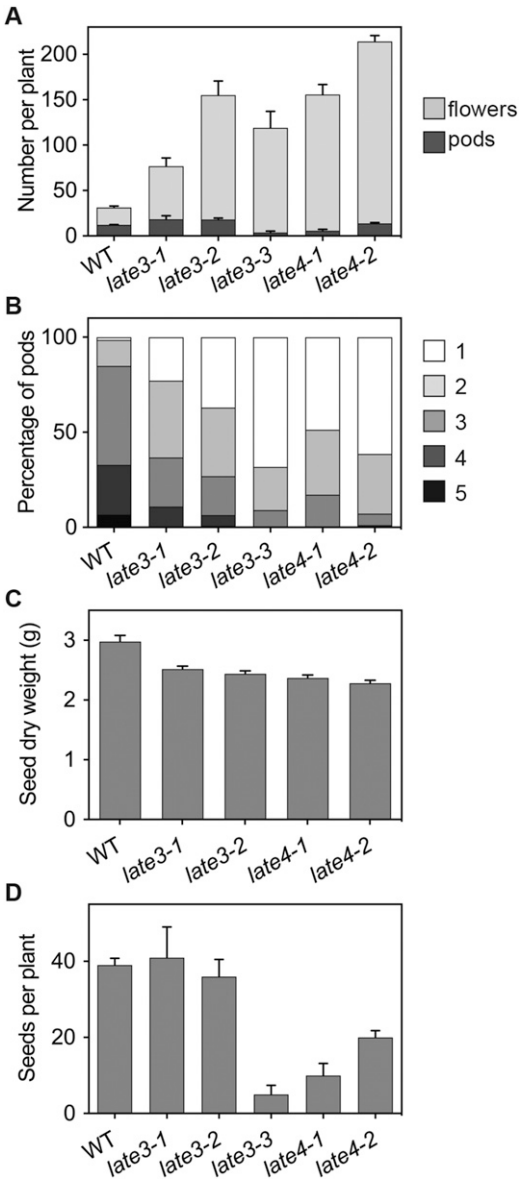

Figure 2. Mutations at *LATE3* and *LATE4* loci affect varied aspects of reproductive development. A, Total number of flowers and pods at maturity. B, Seed content per pod (from one to five seeds) expressed as a proportion of the total number of seed-bearing pods. C, 10-seed dry weight and (D) total number of seeds per plant. Data were collected at the time of harvest and represented as mean ± SE for $n = 6$ (A, B, and D) or $n = 3$ (C).

to wild type, when assessed as the ratio of total branch length to total height at maturity. (Supplemental Fig. S3H; $P < 0.0001$). For individual *late3* and *late4* plants, branching started at around node 11 or 12 and continued for a few nodes, followed by a gap, with branches reappearing just below the node of flower initiation (Supplemental Figs. S1, D and E, and S4). Whereas *late3* mutants showed only aerial branching, we observed both basal and aerial branching for *late4* mutants. Previously, various photoperiod-sensitive and nonsensitive late-flowering mutants were shown to exhibit only basal and aerial branching, respectively (Hecht et al., 2007; Berbel et al., 2012; Sussmilch et al., 2015). Also, whereas wild-type plants typically show an increase in the length of internodes immediately below the node of first open flower (e.g. Weller et al., 1997), this was not seen in the stronger *late3* and *late4* mutants (Supplemental Fig. S3I). Finally, the mutants also showed a delay in the normal progression of compound leaf morphology from one to two pairs of leaflets (Supplemental Fig. S3J) and never progressed to the three-pair stage.

LATE3 and *LATE4* Are Putative Components of the Mediator Complex

Analysis of the F2 progeny of a cross between cv Térèse and late3-1 ($n = 255$) located *LATE3* in a 0.3-cM interval on pea linkage group III (LG III) between markers *BTB1* and *SPS1* (Supplemental Fig. S5A; Supplemental Table S1). The corresponding interval on *Medicago truncatula* chromosome 3 (version 4.0) is 0.9 Mb in length and includes 62 annotated genes (Supplemental Table S1). A similar mapping population (cv Térèse × late4-1 F2; $n = 189$) was used initially to define the position of the *LATE4* locus within a 3.2-cM interval on linkage group V, flanked by markers *MCO1* and *BZIP1* (Supplemental Fig. S5B). Genotyping of further markers within this region in relevant recombinant individuals refined this position to an interval corresponding to a 0.5-Mb region of *M. truncatula* chromosome 7 containing 54 annotated genes (Supplemental Fig. S5C; Supplemental Table S2).

The very close phenotypic similarity between late3 and late4 mutants suggested the possibility that the *LATE3* and *LATE4* genes might encode proteins with complementary functions, potentially acting within the same pathway or protein complex. Therefore, the two regions were scanned for pairs of genes that might be closely related in function. These analyses revealed the presence in both intervals of genes encoding to components of the Mediator transcriptional regulator complex, CYCLIN DEPENDENT KINASE8 (CDK8, Medtr3g096960) and CYCLIN C1 (CYCC1, Medtr7g055650; Supplemental Figs. S6 and S7). This complex is deeply conserved from baker's yeast (*Saccharomyces cerevisiae*) to humans (*Homo sapiens*) and flowering plants and consists of 28 to 34 component proteins that form four distinct modules (Allen and Taatjes, 2015; Jeronimo and Robert, 2017). The CDK8 and CYCC1 proteins associate with two other proteins, MED12 and MED13, to form the so-called CDK8 module (Dolan and Chapple, 2017; Jeronimo and Robert, 2017).

In parallel, RNA sequencing was used to screen transcripts from genes inferred to be within the *LATE3* mapping interval for polymorphisms between *late3-1* and *LATE3* genotypes. Whereas only partial coverage of the transcripts within the region was achieved (Supplemental Table S3), this analysis nevertheless identified a G-to-A mutation typical of ethylmethanesulfonate exposure at position −17 in the 5′ untranslated region (UTR) of the *CDK8* ortholog in *late3-1*, which was verified by Sanger sequencing. This mutation potentially introduces an alternative start codon (GTG/ATG), defining a short (25 amino acid) open reading frame (ORF) out of frame with the *CDK8* coding sequence (Fig. 3A; Supplemental Figs. S8 and S9). Perfect cosegregation of the *PsCDK8* genotype with the *late3* phenotype in the mapping population confirmed the presence of this gene within the defined genetic interval (Supplemental Fig. S4A). Sequencing of PsCDK8 complementary DNA (cDNA) and genomic DNA (gDNA) in *late3-2* and *late3-3* subsequently revealed splice site mutations in both mutants. In *late3-2*, a mutation in the −1 position of the 3′ splice site of intron 12 (AG/AA) resulted in skipping of exon 13 (Fig. 3A; Supplemental Figs. S8 and S9), whereas in *late3-3*, a mutation in the +1 position of the 5′ splice site of intron 4 (GT/AT) resulted in retention of 7 bp from intron 4 in the cDNA, consistent with the activation of an alternative splice site (Fig. 3A; Supplemental Figs. S8 and S9). Both splicing defects were verified by PCR from cDNA using primers specific for either wild type or mutant transcript and would be predicted to result in frameshift and a truncated protein (Supplemental Fig. S9).

In view of these results, the pea *CYCC1* gene (corresponding to transcript PsCam050605) was sequenced

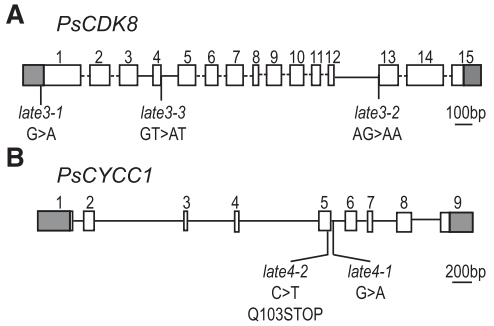

Figure 3. Mutant alleles at *LATE3* and *LATE4* loci carry mutations in genes encoding Mediator complex components CYCLIN-DEPENDENT KINASE8 and CYCLIN C1, respectively. Diagrams showing (A) gene structure of *PsCDK8* and the nature and location of mutations in *late3* alleles and (B) gene structure of *PsCYCC1* and the nature and location of mutations in *late4* alleles. Exons are represented by numbered boxes, with gray shading designating 5′ and 3′ UTRs. Dashed lines in A represent introns not fully characterized. Sequence details of mutations and splice variants are shown in Supplemental Figs. S9, S12, and S13.

from the *late4-1* and *late4-2* mutants. This revealed a nonsense mutation in exon 5, introducing a premature stop codon (Q103X) in *late4-2*, and in *late4-1*, a G-to-A mutation at the +5 position of the 5′ splice site in intron 5 (GTAAGC/GTAAAC; Fig. 3C; Supplemental Figs. S10 and S11). As in the analysis of *CDK8/LATE3*, mapping of *PsCYCC1* confirmed its presence within the defined *LATE4* interval and demonstrated the absence of recombination with the *late4* phenotype in the original mapping population (Supplemental Fig. S4B).

Splicing Defects in *late4* Mutants

Amplification of cDNA from *late4* mutants indicated the presence of multiple bands suggestive of possible splicing variants (Supplemental Fig. S11A). This was confirmed by sequencing of cloned fragments, which identified multiple distinct transcripts with variations around the site of the mutations (Supplemental Fig. S11, B and C). Whereas the majority of transcripts in the *late4-2* mutant were wild type in structure (22 out of 27 clones sequenced), instances of skipping, partial deletion, and partial intron retention involving exon 5 were detected (Fig. 3D; Supplemental Figs. S11 and S12). However, all transcripts would be expected to be nonfunctional, in view of the presence of the *late4-2* nonsense mutation and/or frameshift. In the case of *late4-1*, a small proportion of wild-type transcripts were also detected (3 out of 17), but the majority of transcripts displayed splicing defects around exon 5 (Fig. 3D; Supplemental Figs. S11 and S13), indicative of selection of alternative/cryptic splice sites in preference to the standard site affected by the mutation. All proteins hypothetically encoded by the aberrant transcripts would show significant disruption of the major functional domain of the PsCYCC1 protein, the cyclin N domain, and would therefore likely be inactive.

LATE3 and LATE4 Interact Genetically and Physically

The molecular identities of LATE3 and LATE4 and the similarity of their mutant phenotypes implied their likely genetic and physical interaction. To examine their genetic interaction, we selected *late3-1 late4-2* double mutants. The results in Figure 4, A–C, showed that the double mutant did not differ from the stronger of the two single mutants with respect to either node of flower initiation or leaflet area, indicating that *LATE3* and *LATE4* act in the same genetic pathway. The potential direct physical interaction between LATE3 and LATE4 was then examined using the yeast two-hybrid assay. We found that diploid yeast colonies carrying *PsCDK8* and *PsCYCC1* bait and prey plasmids displayed growth similar to a strong positive interaction control on selective medium (SC-L-W-H+10 mM 3-amino-1,2,4-triazole; Fig. 4D), whereas all negative controls showed no growth. These results indicate that LATE3 and LATE4 also show a strong physical interaction, consistent with

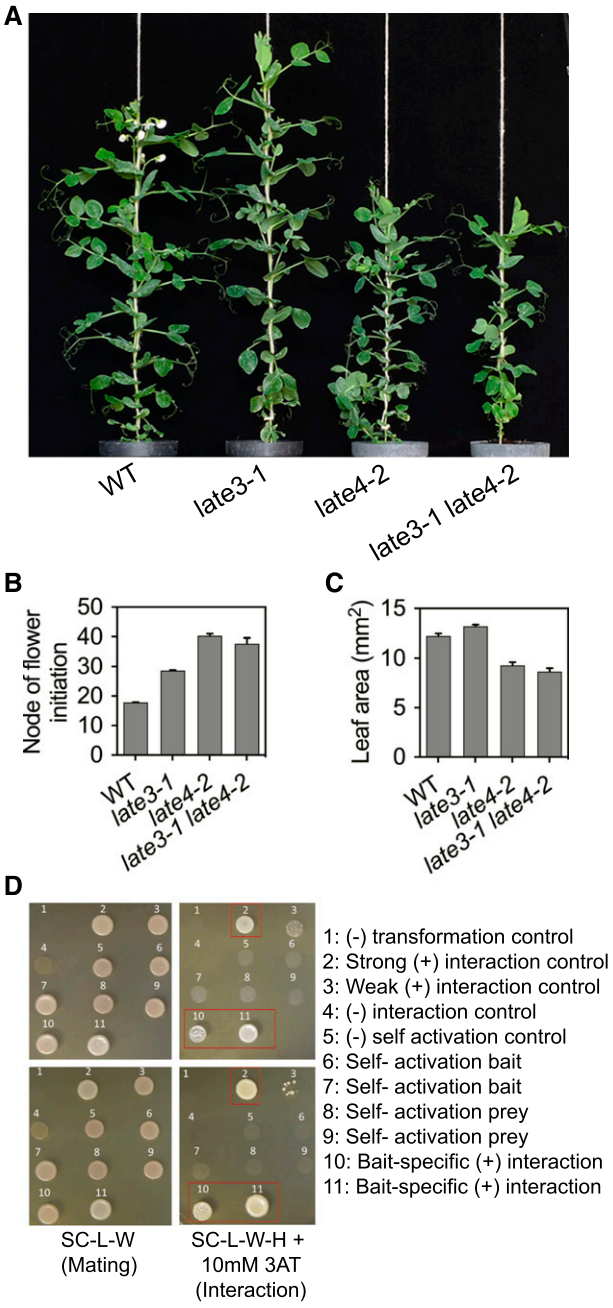

Figure 4. LATE3 and LATE4 show genetic and physical interaction. A to C, Comparison of wild type, *late3-1*, and *late4-2* single mutants and the *late3-1 late4-2* double mutant grown under LD conditions. A, Representative 75-d-old plants. B, Node of flower initiation. C, Representative leaflet area (single leaflet from leaf 10). Data represent mean ± SE for $n = 6$ to 10 plants. D, Yeast two-hybrid analysis for interaction between PsCDK8 and PsCYCC1 proteins from wild-type (NGB5839) genotype. The image shows diploid yeast colonies derived via mating of haploid yeast strains PJ694 alpha and PJ694 A carrying different bait and prey plasmids for experimental and control interactions (as indicated). For each interaction tested, two colonies derived from independent matings (top, colony 1; bottom, colony 2) were used grown in selective interaction-specific (SC-L-W-H +10 mM 3A-amino-1,2,4-triazole [3AT], right) and selective mating-specific (SC-L-W, left) medium and incubated at 30°C for 4 d. Key interactions are highlighted in red.

their molecular identity as components of the same deeply conserved protein complex.

Genetic Interactions between *LATE3* and *LATE4* and Other Flowering Genes

Previous genetic analyses in pea have outlined a genetic pathway for flowering time control (Hecht et al., 2011; Sussmilch et al., 2015; Weller and Ortega, 2015). In an attempt to locate *LATE3* and *LATE4* within this model, we examined the genetic interaction of *late3* and *late4* with two early-flowering mutants, namely *sn* and *lf*. *SN* has primary role as a component of the circadian clock evening complex, which acts to repress flowering and *FT* expression (Liew et al., 2014; Rubenach et al., 2017). *LF* is one of three pea *TFL1* co-orthologs (Foucher et al., 2003), and appears to act downstream of the *FT* gene *FTa1* to repress expression of inflorescence identity genes (Hecht et al., 2011; Sussmilch et al., 2015).

Fig. 5A shows that both *lf late3* and *lf late4* mutants initiated flowering very early and in this respect were much more similar to *lf* single mutants than to *late3* or *late4*. This indicates that the effects of *late3* and *late4* mutations on flower initiation largely depend on the repressive effects of *LF*, although a small but significant increase in flowering node in the double mutants relative to the *lf* single mutant ($P < 0.01$ for both comparisons) indicates that *LATE3* and *LATE4* can also influence the initiation of flowering independently of *LF* to a small extent. In other respects, the double-mutant phenotypes were more similar to *late3* and *late4*, with a massively extended reproductive phase and delayed maturity (Supplemental Fig. S14). In the case of *SN*, we identified plants with *sn late4* genotype as late-flowering segregants in F_3 progeny derived from *sn* individuals in the F2 of a cross between the *sn-4* and *late4-1* mutants. Figure 5B shows that in the presence of *late4*, the *sn* mutation was unable to promote flowering, and *sn late4* plants in fact initiated flowering even later than *late4* single-mutant controls. This suggests that *LATE4* acts downstream of the changes to *FT* expression that are assumed to be the primary cause of the *sn* early-flowering phenotype (Liew et al., 2014; Rubenach et al., 2017).

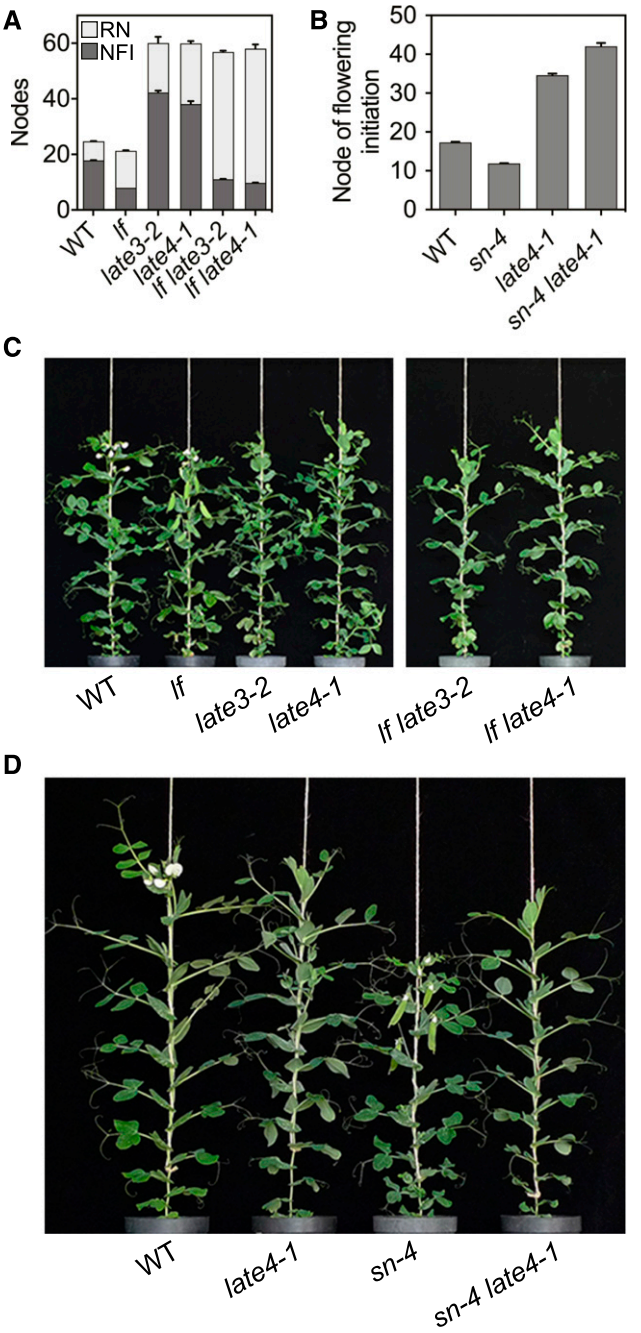

Figure 5. Genetic interactions of *late3* and *late4* mutants with early-flowering mutants *lf* and *sn*. A, Node of flower initiation (NFI) and number of reproductive nodes (RN) in wild-type, *lf*, *late3-2*, *late4-1*, *lf late3-2*, and *lf late4-1* genotypes. B, Node of flower initiation in wild-type, *sn-4*, *late4-1*, and *sn-4 late4-1* genotypes. C and D, Representative plants at 75 (C) and 63 d (D) after sowing. All plants were grown in long days. Data in A and B represent mean ± SE for $n = 6$ to 10 plants.

LATE3 and *LATE4* Regulate Expression of *FT* Genes and Inflorescence-Identity Genes

We next sought to understand how *LATE3* and *LATE4* might regulate the initiation of flowering by examining the effect of *late3* and *late4* mutations on expression of several key flowering-time genes. This analysis focused on the *late3-1* and *late4-1* mutants, which were the only two alleles for which sufficient quantities of seeds were available. Under LD conditions, wild-type and *late3-1* visible flower buds were first detected in dissected apices of wild-type and *late3-1* plants by 42 and 80 d after sowing respectively, whereas *late4-1* mutants did not flower before termination of the experiment. In Arabidopsis, *CDK8* module genes influence the flowering pathway in several different ways, including partially independent effects on *FLC*, *FT*, and *SOC1*/*FUL* expression (Imura et al., 2012).

As *FLC*-like genes are absent from the genomes of pea and related legumes (Hecht et al., 2005), we focused on an analysis of *FT* genes and inflorescence-identity genes.

Previous studies have shown that two of the six pea *FT* genes, *FTa1* and *FTb2*, are induced in leaves under LD, whereas a third gene (*FTc*) is induced at the shoot apex in parallel with inflorescence-identity genes *VEG1* and *PIM* (Hecht et al., 2011; Sussmilch et al., 2015). Figure 6 shows that the expression of the *FTa1* gene in leaves was significantly induced above background by 28 d after sowing in wild-type plants but remained low in *late3* and *late4* mutants. By contrast, the induction of *FTb2* at this same time point was apparently unaffected.

Similar to *FTa1* in leaves, expression of the inflorescence-identity genes *VEG1* and *PIM* in shoot apices was induced by 28 d after sowing in wild-type plants but remained at background levels in *late3* and *late4* mutants, only rising in *late3* at around the time of flower initiation, 10 weeks after sowing. A similar pattern of expression in the shoot apex was also shown by the *LFY* ortholog *UNI* and the apex-specific *FTc* gene. Effects on expression of the *FTa1*, *DET/TFL1a*, and *VEG2/FD* genes were not clear, but *LF/TFL1c* was expressed at a higher level in *late3* and *late4* than in wild type.

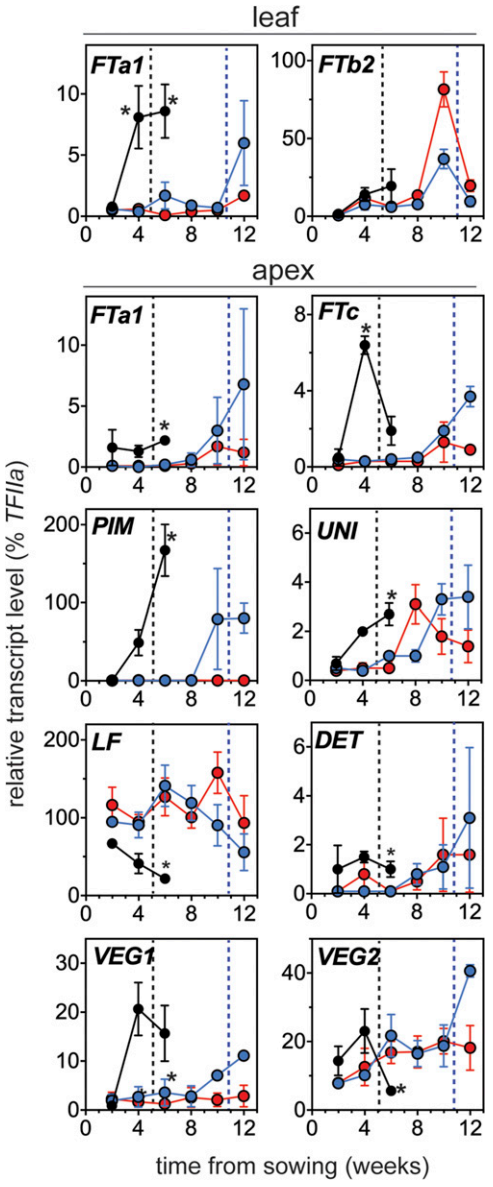

Figure 6. *LATE3* and *LATE4* loci affect expression of several florigen family and inflorescence-identity genes. Developmental time courses for expression of key flowering genes in leaf and shoot apex material from wild type NGB5839 (black), *late3-1* mutant (blue), and *late4-2* mutant (red) grown under long-day conditions. Data have been normalized to the reference gene *TFIIa* and represent mean ± SE for $n = 3$ biological replicates, each consisting of material pooled from two different plants. Black and blue dashed lines indicate the time that flower buds first became visible in dissected shoot apices of wild type and *late3-1* mutants, respectively. Flower initiation did not occur in *late4-1* mutants for the duration of the experiment. Time points at which expression in wild type was significantly different from both mutants ($P \leq 0.05$) are indicated with an asterisk.

DISCUSSION

LATE3 and LATE4 Are Mediator Components

Mapping and sequencing from multiple independent mutant alleles have established the identity of pea flowering-time loci *LATE3* and *LATE4* as the pea orthologs of *CDK8* and *CYCC1*; two genes that encode physically interacting components of the Mediator transcriptional regulation complex. This conclusion is further supported by the very similar pleiotropic phenotypes of *late3* and *late4* mutants and by their genetic and physical interactions.

Mediator is a large and dynamically variable multiprotein complex with diverse and deeply conserved roles in regulation of gene expression from yeast to animals and plants (Allen and Taatjes, 2015; Dolan and Chapple, 2017; Jeronimo and Robert, 2017). It comprises four different modules, of which three (head, tail, and middle) form the so-called "core" Mediator, which has a positive role in general regulation of transcription. The core Mediator forms a preinitiation complex with transcription factors at promoters of target genes, in which it acts to convey signals from gene-specific transcription and to enable the continuous reinitiation of transcription by RNA polymerase II (PolII; Knuesel et al., 2009a). LATE3 and LATE4 are orthologous to components of the fourth, cyclin-dependent kinase module (CKM), which has been shown to bind reversibly with the core Mediator to modify its transcriptional activity (Knuesel et al., 2009a; Allen and Taatjes, 2015).

In plants, a number of different Mediator subunits have been functionally characterized. The first to be described was Arabidopsis PFT1/MED25 (Cerdán and Chory, 2003), which is a component of the middle module of the core Mediator complex. More recently, functional studies have been reported on a number of other core Mediator components, which have been

shown to participate in distinctive ways in diverse processes related to root, shoot, and reproductive development and responses to disease and abiotic stress (Dolan and Chapple, 2017; Kumar et al., 2018; Zhang et al., 2018).

Three of the four subunits of the kinase module (CDK8/CDKE1/HEN3, MED12/CRP/CCT, and MED13/MAB2/GCT) have also been directly functionally characterized in Arabidopsis by analysis of loss-of-function, gain-of-function, and overexpression phenotypes. Mutants have been isolated from several different screens and show diverse defects in embryonic and floral patterning (Wang and Chen, 2004; Gillmor et al., 2010; Ito et al., 2011), developmental phase transitions (Imura et al., 2012; Gillmor et al., 2014), stress and defense responses (Zhu et al., 2014), and hormone signaling (Ito et al., 2011, 2016). The phenotypic effects of the fourth subunit, CYCC1, have not previously been clearly defined (Dolan and Chapple, 2017). This reflects the fact that in Arabidopsis, CYCC1 is present as a recently duplicated tandem pair (Supplemental Fig. S6B), making generation of double mutants by recombination challenging. Zhu et al. (2014) isolated T-DNA-insertion mutants specific for each of these genes but reported no relevant phenotypes, although a mutant with a T-DNA insertion between the two genes showed reduced expression of both genes and some similarities to the defense-related phenotypes of the *cdk8* mutant. Our description of *LATE4* as the single pea ortholog of *CYCC1* and characterization of the *late4-2* nonsense mutant therefore describes the direct consequence of loss of *CYCC1* in plants. We detected no clear phenotypic differences between strong *late3* and *late4* mutants, suggesting that their function is intimately related through essential and complementary roles in the CDK8 module.

Unusual Mutations in *late3* and *late4* Alleles

Among the five mutant alleles characterized in this study, only one, the *late4-2* nonsense mutation, directly affected the coding region. Two others were typical splicing mutations affecting a consensus +1 donor (*late3-3*) or −1 acceptor site (*late3-2*). However, the two remaining mutations were notable for being somewhat less often described.

The *late3-1* mutant carried a single G > A transition at position −17 in the 5′ UTR of CDK8, introducing a novel upstream potential ATG start codon (uATG) and an ORF overlapping and out-of-frame with the canonical CDK8 coding sequence. The most straightforward interpretation is that this uATG might provide an alternative translation initiation site and reduce to some extent the efficiency of translation from the normal AUG (Kozak, 1987). Interference of this nature is known to be greatest when the uORF extends into the major ORF (Kozak, 1987), as seen for *late3-1*. However, relative to the other *late3* and *late4* alleles, the *late3-1* mutant was distinctly less severe (Fig. 1), implying that the wild-type CDK8 ORF is still translated to some extent in *late3-1*. This might in part reflect a weaker context of the upstream initiator codon introduced by the *late3-1* mutation (AAC**A**AAAUG**A**), which retains the conserved A in position −3 but not the G in position +4, whereas both are present in the CDK8 translation initiation site (GCA**A**CCAUG**G**). However, in a recent yeast example, targeted introduction of diverse uAUG revealed effects on both transcription and translation of the associated major ORF that were independent of immediate sequence context (Yun et al., 2012), suggesting the possibility of a broader influence of uAUG beyond simply providing a competing site for initiation of transcription.

The second unusual mutant, *late 4-1*, carried only a single G > A transition at position +5 of the donor site of CYCC1 intron 5, which interferes with normal processing of the CYCC1 transcript (Fig. 3). Although +5 G is highly conserved (>75%) in U2 type GT-AG introns in yeast and animals, genome-wide analyses in Arabidopsis indicate a weaker consensus of around 50% (Sheth et al., 2006; Buratti et al., 2011), and some degree of tolerance for +5 A is therefore likely to explain the presence of normally spliced transcript in *late4-1*. However, the fact that the *late4-1* phenotype appears equivalently severe to that of the *late4-2* nonsense allele (Fig. 1) may therefore suggest that a threshold level of expression is required for CYCC1 function that exceeds that seen in *late4-1*. Although less common by far than mutations affecting the highly conserved +1 and +2 positions, +5 mutations affecting splicing have been described for several human disease genes (e.g. Tran et al., 2005; Fiorentino et al., 2018).

LATE3 and LATE4 Influence Multiple Steps in Flowering Time Control and Reproductive Development

The dramatic effects of *LATE3* and *LATE4* mutations point to a key role for the Mediator kinase module in promotion of flowering and maintenance of diverse aspects of reproductive development. In Arabidopsis, effects of CDK8 and CYCC on flowering have not been examined in detail. However, single mutants for the other two CKM components MED12 and MED13 show similar, relatively strong LD-specific late-flowering phenotypes, again consistent with a close functional relationship (Imura et al., 2012). A weaker late-flowering phenotype has also been reported for an RNA-null CDK8 insertion mutant (Zhu et al., 2014), but this effect has not been further characterized. Thus, based on this relatively limited evidence, it appears that there may be some difference in the relative effects of CKM components on flowering time in Arabidopsis. This is supported by observations from other systems indicating that CKM components, in addition to their co-operative functions, may also function independently to some extent (e.g. Loncle et al., 2007). It also points to a potential difference between pea and Arabidopsis with respect to CDK8 function in flowering time control.

Mutants for *LATE3* and *LATE4* have similar effects on flowering gene expression, with reduced expression

of *GIGAS/FTa1* in leaves and multiple inflorescence-identity genes in the shoot apex. One interpretation of this is that *FTa1* might be the primary target of CKM regulation and that effects on other genes might be a downstream consequence of *FTa1* misregulation, as most are known to be regulated by *FTa1* (Hecht et al., 2011). However, the epistasis of *late4* over *sn*, a mutant in which photoperiod-insensitive early flowering is due to elevated expression of *FTa1* and other *FT* genes in leaves (Liew et al., 2014; Rubenach et al., 2017), suggests that the impaired flowering may not be primarily due to altered *FT* gene expression but because of effects on genes downstream. It is also notable that expression of the *FTb2* gene, which is qualitatively induced by LD in wild-type pea and not detectable in late-flowering photoperiod response mutants (Hecht et al., 2011; Ridge et al., 2016), does not appear to be affected in the *late3* and *late4* mutants (Fig. 6) despite their clear insensitivity to photoperiod for induction of flowering (Fig. 1). This again suggests a primary requirement for CKM in regulation of signaling from *FT* genes, rather than in their regulation.

This interpretation is also consistent with observations that expression of *LF*, a *TFL1* paralog, was elevated in *late3* and *late4* mutants (Fig. 6), and that for initiation of flowering, an *lf* null mutant was epistatic to both *late3* and *late4* (Fig. 5). Formally, this suggests that *LF* is required for expression of the *late3/4* late-flowering phenotype and that the promotion of flowering by the CKM may at least in part involve the transcriptional repression of *LF*. However, the effect of *late3* and *late4* on other aspects of reproductive development in *lf* mutant plants clearly indicates the existence of *LF*-independent effects of CKM action.

No direct information about molecular effects of CDK8 and CYCC1 on flowering time is available from Arabidopsis, but characterization of *med12* and *med13* mutants revealed increased expression of *FLC* and decreased expression of *FT*, *LFY*, and MADS-domain genes *SOC1*, *FUL*, and *AP1* (Imura et al., 2012). In the same study, analysis in *flc* and *ft* mutant backgrounds further established that *MED12* and *MED13* act at multiple steps, with control of *FT* expression partly independent of *FLC* and control of *SOC1* and *FUL* expression at least partly independent of both *FT* and *FLC*. This has been interpreted as a potential feed-forward mechanism that may confer robustness of the flowering transition and is interesting because it supports the idea that the CKM, in addition to its more well-established repressive role, may also activate expression in specific contexts (Nemet et al., 2014). Despite the fact that *FLC* is not present in pea and related legumes, it is still probable that the CKM acts at multiple steps of the flowering and inflorescence-development pathway, including in FT-independent effects on MADS domain genes and other targets.

LATE3 and LATE4 Have Diverse Pleiotropic Effects

Phenotypic effects of *late3* and *late4* mutants beyond flowering and reproductive development indicate that the CDK8 module in pea has pervasive effects throughout development (Figs. 1 and 2; Supplemental Figs. S1–S4). These include effects on stem thickness, leaflet size and shape, seed size and shape, and the timing of changes in compound leaf structure, which has been implicated as a possible marker of vegetative phase change in pea (Wiltshire et al., 1994). These effects are generally similar to those described for Arabidopsis CKM mutants (e.g. Imura et al., 2012; Gillmor et al., 2014; Chhun et al., 2016). This suggests that despite the taxonomic distance between pea and Arabidopsis and despite the fundamental role of the CKM in regulation of gene expression, its preferential involvement in certain aspects of growth and development may be conserved to some extent. This is likely to reflect conservation in the interactions of the CKM with specific transcription factors and corepressors.

In yeast and animal systems, CKM may act by interfering with the positive transcriptional role of the core Mediator complex by blocking its association with PolII, or by directly regulating PolII activity through phosphorylation (Nemet et al., 2014). However, there is also evidence that the CKM can have bidirectional effects on transcription through phosphorylation of transcription factors and may also act independently of core Mediator by direct and indirect modification of histones and regulation of chromatin (Knuesel et al., 2009b; Tsutsui et al., 2013; Allen and Taatjes, 2015). Recent transcriptome analyses have revealed broad effects of Arabidopsis CDK8 on expression of genes involved in processes such as growth regulation, photosynthesis, and light, hormone, defense, and stress responses (Zhu et al., 2014; Mao et al., 2019), but there are few examples in plants where the mechanisms of CKM action have been examined in detail. One recent report has demonstrated the importance of the CDK8 kinase function for some but not all effects on defense-related gene expression (Zhu et al., 2014). Another has linked the CKM to auxin-dependent gene expression through its role in relaying repressive signals from ARF/IAA proteins in association with the TOPLESS corepressor (Ito et al., 2016). Future genomic-scale studies will help define the global effects of the pea CDK8 module and the extent to which they may be shared with Arabidopsis. Such studies should also help clarify the effects of pea CDK8/CYCC1 on flowering-time pathways and shed light on other developmental mechanisms responsible for other aspects of the *late3*/*late4* phenotype. Finally, in view of reports that the Arabidopsis CKM is important for defense and abiotic stress tolerance, it may be of interest to examine the effects of *late3* and *late4* on these traits.

MATERIALS AND METHODS

Plant Materials

The origins of *late3*, *late4*, *lf*, *det*, and *sn-4* mutants in pea (*Pisum sativum*) have been described previously by Foucher et al. (2003) and Hecht et al. (2007). Plants for phenotypic characterizations and genetic analysis (Figs. 1, 2, 4, and 5) were

grown in a glasshouse or phytotron under extended natural daylight, whereas plants for gene expression analysis (Fig. 6) were grown in growth chambers. Growth media, light sources, and growth conditions have been described previously by Hecht et al. (2007). Vernalization treatment was given by subjecting imbibed seeds to 4°C for 4 weeks.

Mapping

Mapping of *LATE3* and *LATE4* utilized a combination of previously described by Aubert et al. (2006) and new gene-based markers, developed from transcript sequences obtained from the pea gene atlas (http://bios.dijon.inra.fr/FATAL/cgi/pscam.cgi) based on sequence comparisons with orthologous genes within syntenic regions of the *Medicago truncatula* genome (Mt4.0v1, https://phytozome.jgi.doe.gov/pz/portal.html#). Marker details are provided in Supplemental Table S3. Linkage analysis was performed using JoinMAP 4 (Kyazma) software.

RNA Sequencing and Data Analysis

RNA sequencing from isogenic *late3-1* and *LATE3* genotypes was performed on RNA pooled from entire embryos isolated from seeds 2 d after imbibition and leaves and shoot apices from 4-week-old plants. Samples were harvested from three plants in two independent replications, and one replication was used for cDNA library construction. Samples from the three different tissues were used for RNA extraction according to SV total RNA isolation (Promega). One microgram of total RNA from each of the three tissues was pooled for preparation and indexing cDNA library using the TruSeq Stranded Total RNA library preparation kit with Ribozero Plant (Illumina). Pools of indexed cDNA libraries of about 260 bp diluted to 6 pM were then used for sequencing in a Miseq next-generation sequencing machine using Miseq Reagent v3 150 cycles kit (Illumina). Quality of the reads generated was assessed in FASTQC in galaxy (Giardine et al., 2005). Paired-end reads were aligned to pea transcript sequences located within the defined interval of *PsLGIII* (Supplemental Table S3) in Geneious 8.0.4 software.

Other Molecular Analyses

PCR fragments were purified using Promega Wizard SV gel and PCR clean-up system (Promega) and cloned using pGEM-T easy vector (Promega) by following manufacturer's protocol. Sequencing was performed at Macrogen. For gene expression assays, both leaflets from the second youngest fully expanded leaf and a dissected apical bud containing the shoot apex (~2 mm in length) were harvested from two plants per replicate. These samples were frozen in liquid nitrogen and processed for RNA extraction, reverse transcription, and reverse transcription quantitative PCR, according to procedures described previously by Sussmilch et al. (2015). Two technical and three biological replicates were used for each sample point. Details of primers are given in Supplemental Table S3.

Phylogenetic Analysis

Phylogenetic analysis was performed by identification of genes through BLAST searches of the *M. truncatula* genome (Mt4.0v1) and pea gene atlas with reciprocal BLAST searches against the Arabidopsis genome at TAIR (www.arabidopsis.org) to confirm gene identity. Full-length amino acid sequences were aligned using ClustalX (Thompson et al., 1997), adjusted manually, and analyzed using distance based methods in PAUP* (Supplemental Figs. S6, S7, and S10).

Yeast Two-Hybrid Assay

Full-length coding sequences of *PsCDK8* and *PsCYCC1* were amplified from wild-type (NGB5839) cDNA, cloned into yeast two-hybrid destination vectors, and tested for interactions following methods described previously by Ridge et al. (2016). Empty vector controls were performed to test, and controls for strong and negative interactions provided as part of the ProQuest two-hybrid system were performed according to the manufacturer's instructions. Relevant details of primers and constructs are listed in Supplemental Tables S4 and S5.

Statistical Analysis

For statistical analysis of data presented in Figures 1, 2, and 4, Welch *t* test (two tailed) with 95% confidence interval was performed, whereas for Figure 6, a one-way ANOVA followed by Dunnett test was used. Analyses were conducted in GraphPad Prism (v7, GraphPad Software).

Accession Numbers

Sequences referred to in this article can be found in the *P. sativum* v1a genome database (urgi.versailles.inra.fr) under loci Psat5g058480/PsCam048317 (*PsCDK8/LATE3*) and Psat3g149520/PsCam050605 (*PsCYCC1/LATE4*).

Supplemental Data

The following supplemental materials are available.

Supplemental Figure S1. Inflorescence development and reversion in *late3* and *late4* mutants.

Supplemental Figure S2. Pod and seed morphology in *late3* and *late4* mutants.

Supplemental Figure S3. Effect of and *late3* and *late4* mutations on vegetative growth traits.

Supplemental Figure S4. Diagram illustrating branching pattern in *late3* and *late4* mutants.

Supplemental Figure S5. Genetic mapping of *LATE3 and LATE4* loci.

Supplemental Figure S6. Phylogenetic trees showing identity and relationships of PsCDK8 and PsCYCC1 protein sequences.

Supplemental Figure S7. Alignment of CDK8 protein sequences.

Supplemental Figure S8. Alternative splicing and putative ORF generation for wild-type and *late3* mutant alleles of *PsCDK8*.

Supplemental Figure S9. Sites and consequences of mutations in *PsCDK8* in *late3* mutant alleles.

Supplemental Figure S10. Alignment of CYCC1 protein sequences.

Supplemental Figure S11. Alternative splicing and putative ORF generation for wild-type and *late4* mutant alleles of *PsCYCC1*.

Supplemental Figure S12. Sites of mutations in *PsCYCC1* in *late4* mutant alleles and consequences for splicing in *late4-2*.

Supplemental Figure S13. Consequences of the *late4-1* mutation for splicing of *PsCYCC1*.

Supplemental Figure S14. Genetic interaction of *late3-2* and *late4-1* mutants with *lf-22* and *det* mutants.

Supplemental Table S1. Details of gene-based markers used for mapping of *LATE3* and their *Medicago* orthologs.

Supplemental Table S2. Details of gene-based markers used for mapping of *LATE4* and their *Medicago* orthologs.

Supplemental Table S3. Comparison of RNA sequencing data analysis for pea transcriptome sequences inferred by mapping and/or synteny with *Medicago* to derive from genes located in the mapping interval for *LATE3* (*BTB1-SPS1* in PsLGIII).

Supplemental Table S4. Primer details.

Supplemental Table S5. Details of bait and prey plasmids used in yeast two hybrid assays for testing interactions between pea CDK8 and CYCC1 proteins.

ACKNOWLEDGMENTS

We thank Ian Cummings, Michelle Lang, and Tracey Winterbottom for help with plant husbandry.

Received September 24, 2019; accepted November 26, 2019; published January 21, 2020.

LITERATURE CITED

Allen BL, Taatjes DJ (2015) The Mediator complex: A central integrator of transcription. Nat Rev Mol Cell Biol **16:** 155–166

Andrés F, Coupland G (2012) The genetic basis of flowering responses to seasonal cues. Nat Rev Genet **13:** 627–639

Aubert G, Morin J, Jacquin F, Loridon K, Quillet MC, Petit A, Rameau C, Lejeune-Hénaut I, Huguet T, Burstin J (2006) Functional mapping in pea, as an aid to the candidate gene selection and for investigating synteny with the model legume *Medicago truncatula*. Theor Appl Genet **112:** 1024–1041

Berbel A, Ferrándiz C, Hecht V, Dalmais M, Lund OS, Sussmilch FC, Taylor SA, Bendahmane A, Ellis TH, Beltrán JP, et al (2012) VEGETATIVE1 is essential for development of the compound inflorescence in pea. Nat Commun **3:** 797

Blümel M, Dally N, Jung C (2015) Flowering time regulation in crops—what did we learn from *Arabidopsis*? Curr Opin Biotechnol **32:** 121–129

Brambilla V, Martignago D, Goretti D, Cerise M, Somssich M, de Rosa M, Galbiati F, Shrestha R, Lazzaro F, Simon R, et al (2017) Antagonistic transcription factor complexes modulate the floral transition in rice. Plant Cell **29:** 2801–2816

Bratzel F, Turck F (2015) Molecular memories in the regulation of seasonal flowering: From competence to cessation. Genome Biol **16:** 192

Buratti E, Chivers M, Hwang G, Vorechovsky I (2011) DBASS3 and DBASS5: Databases of aberrant 3′- and 5′-splice sites. Nucleic Acids Res **39:** D86–D91

Cai Y, Chen L, Liu X, Guo C, Sun S, Wu C, Jiang B, Han T, Hou W (2018) CRISPR/Cas9-mediated targeted mutagenesis of *GmFT2a* delays flowering time in soya bean. Plant Biotechnol J **16:** 176–185

Cao D, Takeshima R, Zhao C, Liu B, Jun A, Kong F (2017) Molecular mechanisms of flowering under long days and stem growth habit in soybean. J Exp Bot **68:** 1873–1884

Causier B, Ashworth M, Guo W, Davies B (2012) The TOPLESS interactome: A framework for gene repression in Arabidopsis. Plant Physiol **158:** 423–438

Cerdán PD, Chory J (2003) Regulation of flowering time by light quality. Nature **423:** 881–885

Chhun T, Chong SY, Park BS, Wong ECC, Yin JL, Kim M, Chua NH (2016) HSI2 repressor recruits MED13 and HDA6 to down-regulate seed maturation gene expression directly during Arabidopsis early seedling growth. Plant Cell Physiol **57:** 1689–1706

Cho LH, Yoon J, An G (2017) The control of flowering time by environmental factors. Plant J **90:** 708–719

Dolan WL, Chapple C (2017) Conservation and divergence of mediator structure and function: Insights from plants. Plant Cell Physiol **58:** 4–21

Eom H, Park SJ, Kim MK, Kim H, Kang H, Lee I (2018) TAF15b, involved in the autonomous pathway for flowering, represses transcription of *FLOWERING LOCUS C*. Plant J **93:** 79–91

Fiorentino A, Yu J, Arno G, Pontikos N, Halford S, Broadgate S, Michaelides M, Carss KJ, Raymond FL, Cheetham ME, et al; NIHR-BioResource Rare Diseases Consortium; U.K. Inherited Retinal Dystrophy Consortium (2018) Novel homozygous splicing mutations in *ARL2BP* cause autosomal recessive retinitis pigmentosa. Mol Vis **24:** 603–612

Fjellheim S, Boden S, Trevaskis B (2014) The role of seasonal flowering responses in adaptation of grasses to temperate climates. Front Plant Sci **5:** 431

Foucher F, Morin J, Courtiade J, Cadioux S, Ellis N, Banfield MJ, Rameau C (2003) *DETERMINATE* and *LATE FLOWERING* are two *TERMINAL FLOWER1/CENTRORADIALIS* homologs that control two distinct phases of flowering initiation and development in pea. Plant Cell **15:** 2742–2754

Giardine B, Riemer C, Hardison RC, Burhans R, Elnitski L, Shah P, Zhang Y, Blankenberg D, Albert I, Taylor J, et al (2005) Galaxy: A platform for interactive large-scale genome analysis. Genome Res **15:** 1451–1455

Gillmor CS, Park MY, Smith MR, Pepitone R, Kerstetter RA, Poethig RS (2010) The MED12-MED13 module of Mediator regulates the timing of embryo patterning in *Arabidopsis*. Development **137:** 113–122

Gillmor CS, Silva-Ortega CO, Willmann MR, Buendía-Monreal M, Poethig RS (2014) The *Arabidopsis* Mediator *CDK8* module genes *CCT* (*MED12*) and *GCT* (*MED13*) are global regulators of developmental phase transitions. Development **141:** 4580–4589

Hecht V, Foucher F, Ferrándiz C, Macknight R, Navarro C, Morin J, Vardy ME, Ellis N, Beltrán JP, Rameau C, et al (2005) Conservation of *Arabidopsis* flowering genes in model legumes. Plant Physiol **137:** 1420–1434

Hecht V, Knowles CL, Vander Schoor JK, Liew LC, Jones SE, Lambert MJ, Weller JL (2007) Pea *LATE BLOOMER1* is a *GIGANTEA* ortholog with roles in photoperiodic flowering, deetiolation, and transcriptional regulation of circadian clock gene homologs. Plant Physiol **144:** 648–661

Hecht V, Laurie RE, Vander Schoor JK, Ridge S, Knowles CL, Liew LC, Sussmilch FC, Murfet IC, Macknight RC, Weller JL (2011) The pea GIGAS gene is a FLOWERING LOCUS T homolog necessary for graft-transmissible specification of flowering but not for responsiveness to photoperiod. Plant Cell **23:** 147–161

Higuchi Y (2018) Florigen and anti-florigen: Flowering regulation in horticultural crops. Breed Sci **68:** 109–118

Imura Y, Kobayashi Y, Yamamoto S, Furutani M, Tasaka M, Abe M, Araki T (2012) *CRYPTIC PRECOCIOUS/MED12* is a novel flowering regulator with multiple target steps in *Arabidopsis*. Plant Cell Physiol **53:** 287–303

Ito J, Fukaki H, Onoda M, Li L, Li C, Tasaka M, Furutani M (2016) Auxin-dependent compositional change in Mediator in ARF7- and ARF19-mediated transcription. Proc Natl Acad Sci USA **113:** 6562–6567

Ito J, Sono T, Tasaka M, Furutani M (2011) *MACCHI-BOU 2* is required for early embryo patterning and cotyledon organogenesis in *Arabidopsis*. Plant Cell Physiol **52:** 539–552

Jeronimo C, Robert F (2017) The mediator complex: At the nexus of RNA polymerase II transcription. Trends Cell Biol **27:** 765–783

Knuesel MT, Meyer KD, Bernecky C, Taatjes DJ (2009a) The human CDK8 subcomplex is a molecular switch that controls Mediator coactivator function. Genes Dev **23:** 439–451

Knuesel MT, Meyer KD, Donner AJ, Espinosa JM, Taatjes DJ (2009b) The human CDK8 subcomplex is a histone kinase that requires Med12 for activity and can function independently of mediator. Mol Cell Biol **29:** 650–661

Kozak M (1987) An analysis of 5′-noncoding sequences from 699 vertebrate messenger RNAs. Nucleic Acids Res **15:** 8125–8148

Kumar KRR, Blomberg J, Björklund S (2018) The *MED7* subunit paralogs of Mediator function redundantly in development of etiolated seedlings in *Arabidopsis*. Plant J **96:** 578–594

Laurie RE, Diwadkar P, Jaudal M, Zhang L, Hecht V, Wen J, Tadege M, Mysore KS, Putterill J, Weller JL, et al (2011) The Medicago *FLOWERING LOCUS T* homolog, *MtFTa1*, is a key regulator of flowering time. Plant Physiol **156:** 2207–2224

Liew LC, Hecht V, Sussmilch FC, Weller JL (2014) the pea photoperiod response gene *STERILE NODES* is an ortholog of *LUX ARRHYTHMO*. Plant Physiol **165:** 648–657

Loncle N, Boube M, Joulia L, Boschiero C, Werner M, Cribbs DL, Bourbon HM (2007) Distinct roles for Mediator Cdk8 module subunits in *Drosophila* development. EMBO J **26:** 1045–1054

Luo X, Gao Z, Wang Y, Chen Z, Zhang W, Huang J, Yu H, He Y (2018) The NUCLEAR FACTOR-CONSTANS complex antagonizes Polycomb repression to de-repress *FLOWERING LOCUS T* expression in response to inductive long days in *Arabidopsis*. Plant J **95:** 17–29

Mao X, Kim JI, Wheeler MT, Heintzelman AK, Weake VM, Chapple C (2019) Mutation of Mediator subunit *CDK8* counteracts the stunted growth and salicylic acid hyperaccumulation phenotypes of an *Arabidopsis MED5* mutant. New Phytol **223:** 233–245

Nemet J, Jelicic B, Rubelj I, Sopta M (2014) The two faces of Cdk8, a positive/negative regulator of transcription. Biochimie **97:** 22–27

Ridge S, Sussmilch FC, Hecht V, Vander Schoor JK, Lee R, Aubert G, Burstin J, Macknight RC, Weller JL (2016) Identification of *LATE BLOOMER2* as a *CYCLING DOF FACTOR* homolog reveals conserved and divergent features of the flowering response to photoperiod in pea. Plant Cell **28:** 2545–2559

Rubenach AJ, Hecht V, Vander Schoor JK, Liew LC, Aubert G, Burstin J, Weller JL (2017) *EARLY FLOWERING3* redundancy fine-tunes photoperiod sensitivity. Plant Physiol **173:** 2253–2264

Sheth N, Roca X, Hastings ML, Roeder T, Krainer AR, Sachidanandam R (2006) Comprehensive splice-site analysis using comparative genomics. Nucleic Acids Res **34:** 3955–3967

Shi J, Dong A, Shen WH (2015) Epigenetic regulation of rice flowering and reproduction. Front Plant Sci **5:** 803

Shim JS, Kubota A, Imaizumi T (2017) Circadian clock and photoperiodic flowering in *Arabidopsis*: CONSTANS is a hub for signal integration. Plant Physiol **173:** 5–15

Song YH, Shim JS, Kinmonth-Schultz HA, Imaizumi T (2015) Photoperiodic flowering: time measurement mechanisms in leaves. Annu Rev Plant Biol **66:** 441–464

Sussmilch FC, Berbel A, Hecht V, Vander Schoor JK, Ferrándiz C, Madueño F, Weller JL (2015) Pea *VEGETATIVE2* is an *FD* homolog that is essential for flowering and compound inflorescence development. Plant Cell **27:** 1046–1060

Thompson JD, Gibson TJ, Plewniak F, Jeanmougin F, Higgins DG (1997) The CLUSTAL_X windows interface: Flexible strategies for multiple sequence alignment aided by quality analysis tools. Nucleic Acids Res **25:** 4876–4882

Tran VK, Zhang Z, Yagi M, Nishiyama A, Habara Y, Takeshima Y, Matsuo M (2005) A novel cryptic exon identified in the 3′ region of intron 2 of the human dystrophin gene. J Hum Genet **50:** 425–433

Tsutsui T, Fukasawa R, Shinmyouzu K, Nakagawa R, Tobe K, Tanaka A, Ohkuma Y (2013) Mediator complex recruits epigenetic regulators via its two cyclin-dependent kinase subunits to repress transcription of immune response genes. J Biol Chem **288:** 20955–20965

Wagner D (2017) Key developmental transitions during flower morphogenesis and their regulation. Curr Opin Genet Dev **45:** 44–50

Wang W, Chen X (2004) *HUA ENHANCER3* reveals a role for a cyclin-dependent protein kinase in the specification of floral organ identity in Arabidopsis. Development **131:** 3147–3156

Weller JL, Ortega R (2015) Genetic control of flowering time in legumes. Front Plant Sci **6:** 207

Weller JL, Reid JB, Taylor SA, Murfet IC (1997) The genetic control of flowering in pea. Trends Plant Sci **2:** 412–418

Whittaker C, Dean C (2017) The *FLC* locus: A platform for discoveries in epigenetics and adaptation. Annu Rev Cell Dev Biol **33:** 555–575

Wigge PA, Kim MC, Jaeger KE, Busch W, Schmid M, Lohmann JU, Weigel D (2005) Integration of spatial and temporal information during floral induction in *Arabidopsis*. Science **309:** 1056–1059

Wiltshire RJE, Murfet IC, Reid JB (1994) The genetic control of heterochrony: Evidence from developmental mutants of *Pisum sativum* L. J Evol Biol **7:** 447–465

Yun Y, Adesanya TM, Mitra RD (2012) A systematic study of gene expression variation at single-nucleotide resolution reveals widespread regulatory roles for uAUGs. Genome Res **22:** 1089–1097

Zhang X, Zhou W, Chen Q, Fang M, Zheng S, Scheres B, Li C (2018) Mediator subunit MED31 is required for radial patterning of *Arabidopsis* roots. Proc Natl Acad Sci USA **115:** E5624–E5633

Zhu Y, Schluttenhoffer CM, Wang P, Fu F, Thimmapuram J, Zhu JK, Lee SY, Yun DJ, Mengiste T (2014) CYCLIN-DEPENDENT KINASE8 differentially regulates plant immunity to fungal pathogens through kinase-dependent and -independent functions in Arabidopsis. Plant Cell **26:** 4149–4170